Effective medium theories for irregular fluffy structures: aggregation of small particles

Nikolai V. Voshchinnikov,[1,*] Gorden Videen,[2] and Thomas Henning[3]

[1]Sobolev Astronomical Institute, St. Petersburg University, St. Petersburg 198504, Russia
[2]U.S. Army Research Laboratory, AMSRD-ARL-CI-ES, 2800 Powder Mill Road, Adelphi, Maryland 20783
[3]Max-Planck-Institut für Astronomie, Königstuhl 17, D-69117 Heidelberg, Germany

*Corresponding author: nvv@astro.spbu.ru

Received 31 October 2006; revised 9 February 2007; accepted 16 February 2007;
posted 21 February 2007 (Doc. ID 76312); published 12 June 2007

The extinction efficiencies as well as the scattering properties of particles of different porosity are studied. Calculations are performed for porous pseudospheres with small size (Rayleigh) inclusions using the discrete dipole approximation. Five refractive indices of materials covering the range from $1.20 + 0.00i$ to $1.75 + 0.58i$ were selected. They correspond to biological particles, dirty ice, silicate, and amorphous carbon and soot in the visual part of the spectrum. We attempt to describe the optical properties of such particles using Lorenz–Mie theory and a refractive index found from some effective medium theory (EMT) assuming the particle is homogeneous. We refer to this as the effective model. It is found that the deviations are minimal when utilizing the EMT based on the Bruggeman mixing rule. Usually the deviations in the extinction factor do not exceed ~5% for particle porosity $\mathcal{P} = 0 - 0.9$ and size parameters $x_{\mathrm{porous}} = 2\pi r_{\mathrm{s,porous}}/\lambda \lesssim 25$. The deviations are larger for scattering and absorption efficiencies and smaller for particle albedo and the asymmetry parameter. Our calculations made for spheroids confirm these conclusions. Preliminary consideration shows that the effective model represents the intensity and polarization of radiation scattered by fluffy aggregates quite well. Thus the effective models of spherical and nonspherical particles can be used to significantly simplify the computations of the optical properties of aggregates containing only Rayleigh inclusions.

OCIS codes: 290.0290, 290.5850.

1. Introduction

Fluffy aggregate particles are encountered in the atmosphere and ocean, interstellar clouds, and biological and chemical media. Finding their optical properties is an important task for different fields of science and industry. Great progress in the theoretical study of the light scattered by small particles discerned in the last several years makes it possible to calculate the optical properties of arbitrary-shaped particles with anisotropic optical properties and inclusions [1]. However, a major part of the numerical techniques developed for aggregates is still computationally intensive. Moreover, the real structures of scatterers are poorly known, making detailed calculations often impossible. Therefore it is attractive to find a way to treat the optics of large fluffy particles using simplified models; for example, to replace the aggregates by some simplified homogeneous particles with some average dielectric function. [The approach is called the effective medium theory (EMT), see Refs. 2 and 3 for discussion.]

There are many different mixing rules for dielectric functions (see, e.g., Refs. 4–6). They are rediscovered from time to time and sometimes one effective medium expression can be derived from another one. The EMTs for mixtures of materials are traditionally considered within the framework of electrostatic fields [4]. Evidently, this restricts the range of applicability of the EMTs. Note that previous considerations were given to small volume fractions of inclusions in particles (≲20%–40%).

In this paper we consider particles consisting of vacuum and some material. We analyze the optical properties of aggregate particles using the discrete dipole approximation (DDA) [7] and compare them

0003-6935/07/194065-08$15.00/0

with results using effective models; e.g., for porous pseudospheres the scattering properties are determined assuming the sphere is homogeneous, and its refractive index is determined with an EMT. The porosity is varied up to 90%, which corresponds to very fluffy particles resembling aggregates with a fractal dimension <2 (see, e.g., Ref. 8).

Some results for three-component composite particles (silicate, carbon, and vacuum) have already been presented by Voshchinnikov *et al*. [9]. They show that the EMT approach can give rather accurate results only if very porous particles have so-called Rayleigh inclusions (small in comparison with the wavelength of incident radiation). At the same time, the optical properties of heterogeneous spherical particles having inclusions of various sizes (Rayleigh and non-Rayleigh) and very large porosity are found to resemble those of spheres with a large number ($\gtrsim$15–20) of different layers.

The particle models are described in Section 2. In Section 3 we present some illustrative results using the effective model, size, and refractive index of inclusions and particle shape variations. Concluding remarks are given in Section 4.

2. Models of Particles and Calculations

We consider spherical particles consisting of some amount of a material and some amount of vacuum. The amount of vacuum characterizes the particle porosity $\mathcal{P}$ ($0 \le \mathcal{P} < 1$), which is introduced as

$$\mathcal{P} = V_{\mathrm{vac}}/V_{\mathrm{total}} = 1 - V_{\mathrm{solid}}/V_{\mathrm{total}}, \tag{1}$$

where V_{vac} and V_{solid} are the volume fractions of vacuum and solid material, respectively. If $\mathcal{P} = 0$ the particle is homogeneous and compact, and its optical properties are described by the Lorenz–Mie theory. If the porosity is small we can consider the particle as a solid matrix with vacuum inclusions. If the porosity is large (the case of very fluffy aggregates) the particle can be presented as a vacuum matrix with solid inclusions. For aggregates the porosity can be represented as unity minus the volume fraction of solid material in a sphere described around the aggregate. Fluffy particles also can be presented as homogeneous spheres of the same material mass with a refractive index found using an EMT. The size parameter of porous particles can be found as

$$x_{\mathrm{porous}} = \frac{2\pi r_{\mathrm{s,porous}}}{\lambda} = \frac{x_{\mathrm{compact}}}{(1-\mathcal{P})^{1/3}} = \frac{x_{\mathrm{compact}}}{(V_{\mathrm{solid}}/V_{\mathrm{total}})^{1/3}}. \tag{2}$$

Thus, $x_{\mathrm{porous}} = x_{\mathrm{compact}}$ if $\mathcal{P} = 0$.

A. Discrete Dipole Approximation Calculations

The calculations of the optical properties of particles with inclusions are performed with the DDA. We use the version DDSCAT 6.0 developed by Draine and Flatau [10]. This technique can treat particles of arbitrary shape and inhomogeneous structure.

The particles ("targets" in DDSCAT terminology) are constructed employing a special routine producing quasi-spherical targets with cubic inclusions of a fixed size. The sizes of the target d_{max} and of the inclusions d_{incl} are expressed in units of the interdipole distance d.

In contrast to previous modeling efforts (e.g., Refs. 11–13), porous particles are not produced by removing dipoles or inclusions from a target but by attributing the refractive index $m = 1.000001 + 0.0i$ to the vacuum.

For the purpose of treating very porous particles, the number of dipoles in the pseudospheres is taken to be quite large. In all cases considered, particles with maximum size $d_{\mathrm{max}} = 91$ are studied. This value corresponds to the total number of dipoles in pseudospheres $N_{\mathrm{dip}} = 357128$–$381915$ depending on the size of inclusions d_{incl}. Thus the criterion of the validity of the DDA for calculations of the extinction/scattering cross sections $|m|kd < 1$ ($m = n + ki$ is the complex refractive index of the material, see Section 3 for its choice, $k = 2\pi/\lambda$ the wavenumber with λ being the wavelength in vacuum) of Draine and Flatau [10] is satisfied up to size parameter $x_{\mathrm{porous}} \approx 27$–$40$.

Targets with randomly distributed cubic inclusions with values of d_{incl} ranging from 1 to 5 are considered. Note that the inclusions of the size $d_{\mathrm{incl}} = 1$ are dipoles, while the inclusions with $d_{\mathrm{incl}} = 3$ and 5 consist of 27 and 125 dipoles, respectively. The optical characteristics of pseudospheres with inclusions are averaged over three targets obtained for different random number sets. The calculations show that in our case such an approach is practically equivalent to time-consuming numerical averaging over target orientations.

B. Effective Medium Theory Calculations

An EMT allows one to determine an effective dielectric function $\varepsilon_{\mathrm{eff}}$ (the dielectric permittivity is related to the refractive index as $\varepsilon = m^2$) of any heterogeneous particle consisting of several materials with dielectric functions ε_i. EMTs are utilized extensively in optics of inhomogeneous media (see the discussion

Table 1. Mixing Rules for the Refractive Indices

Mixing Rule	Formula
Bruggeman	$f\frac{\varepsilon_1 - \varepsilon_{\mathrm{eff}}}{\varepsilon_1 + 2\varepsilon_{\mathrm{eff}}} + (1-f)\frac{\varepsilon_2 - \varepsilon_{\mathrm{eff}}}{\varepsilon_2 + 2\varepsilon_{\mathrm{eff}}} = 0$
Garnett	$\varepsilon_{\mathrm{eff}} = \varepsilon_2\left[1 + \frac{3f\frac{\varepsilon_1 - \varepsilon_2}{\varepsilon_1 + 2\varepsilon_2}}{1 - f\frac{\varepsilon_1 - \varepsilon_2}{\varepsilon_1 + 2\varepsilon_2}}\right]$
Inverse Garnett	$\varepsilon_{\mathrm{eff}} = \varepsilon_1\left[1 + \frac{3(1-f)\frac{\varepsilon_2 - \varepsilon_1}{\varepsilon_2 + 2\varepsilon_1}}{1 - (1-f)\frac{\varepsilon_2 - \varepsilon_1}{\varepsilon_2 + 2\varepsilon_1}}\right]$
Looyenga	${\varepsilon_{\mathrm{eff}}}^{1/3} = f{\varepsilon_1}^{1/3} + (1-f){\varepsilon_2}^{1/3}$
Birchak	${\varepsilon_{\mathrm{eff}}}^{1/2} = f{\varepsilon_1}^{1/2} + (1-f){\varepsilon_2}^{1/2}$
Lichtenecker	$\log \varepsilon_{\mathrm{eff}} = f \log \varepsilon_1 + (1-f)\log \varepsilon_2$

in Refs. 4, 14–17 and the references therein). However, full systematic studies of the accuracy of different mixing rules are lacking.

In this work we study several EMTs including the two most often used, the Bruggeman and Garnett EMTs. The formulas of mixing rules are collected in Table 1 (f is the volume fraction of component 1), and corresponding references can be found in Refs. 6 and 18. We usually consider that $f = V_{\mathrm{solid}}/V_{\mathrm{total}}$ and $1 - f = V_{\mathrm{vac}}/V_{\mathrm{total}}$. Note also that the Garnett rule assumes that one material is a matrix (host material) in which the other material is embedded. When the roles of the inclusion and the host material are reversed, the inverse Garnett rule is obtained.

3. Numerical Results and Discussion

Here we present the results illustrating the behavior of the efficiency factors or cross sections. We consider primarily the extinction efficiency factor $Q_{\mathrm{ext}} = C_{\mathrm{ext}}/\pi r_s^2$, where C_{ext} is the extinction cross section and r_s the radius of the spherical particle. The refractive indices of compact particles are chosen to be $m_{\mathrm{compact}} = 1.20 + 0.00i$, $m_{\mathrm{compact}} = 1.33 + 0.01i$, $m_{\mathrm{compact}} = 1.68 + 0.03i$, $m_{\mathrm{compact}} = 1.98 + 0.23i$, and $m_{\mathrm{compact}} = 1.75 + 0.58i$. These values are typical of the refractive indices of biological particles, dirty ice, silicate, and amorphous carbon, and soot in the visual part of the spectrum, respectively. The refractive indices are taken from the Jena-Petersburg Database of Optical Constants (JPDOC) described in Refs. 19 and 20 (for soot we used the data published in Ref. 21).

A. Effect of the Size of Inclusions

The size of constituent particles (inclusions) is an important parameter influencing light scattering by aggregates. In Ref. 9 it was demonstrated that the Lorenz–Mie theory together with the standard EMTs (Garnett or Bruggeman) reproduces the optical properties of aggregates for particles with small (Rayleigh) inclusions only. If the inclusions are not simple

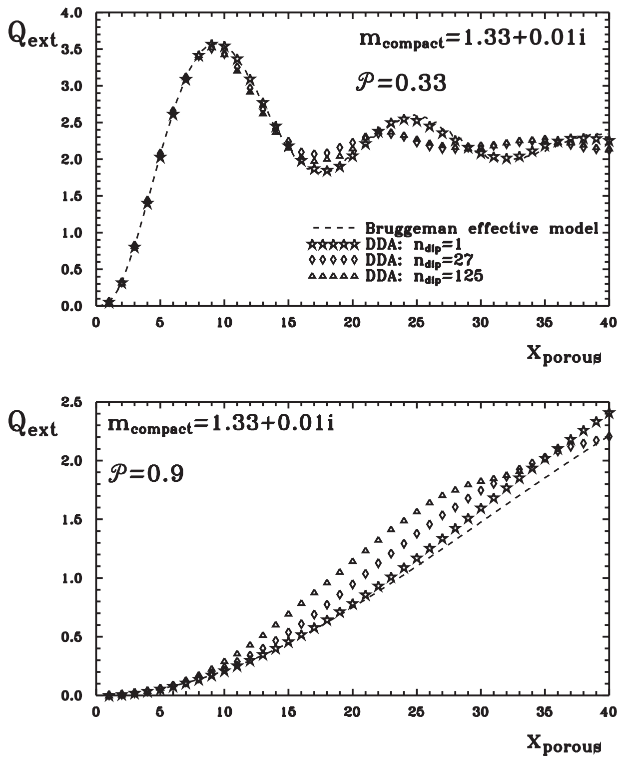

Fig. 1. Size dependence of the extinction efficiency factors calculated for spheres with inclusions of different sizes (DDA computations) and with the Lorenz–Mie theory using the Bruggeman EMT. The refractive index of inclusions is $m_{\mathrm{compact}} = 1.33 + 0.01i$. The effective refractive indices of porous particles are indicated in Table 3. The porosity of particles is $\mathcal{P} = 0.33$ (upper panel) and $\mathcal{P} = 0.9$ (lower panel). For a given porosity the particles of the same size parameter x_{porous} have the same mass. The effect of variations of the size of inclusions is illustrated.

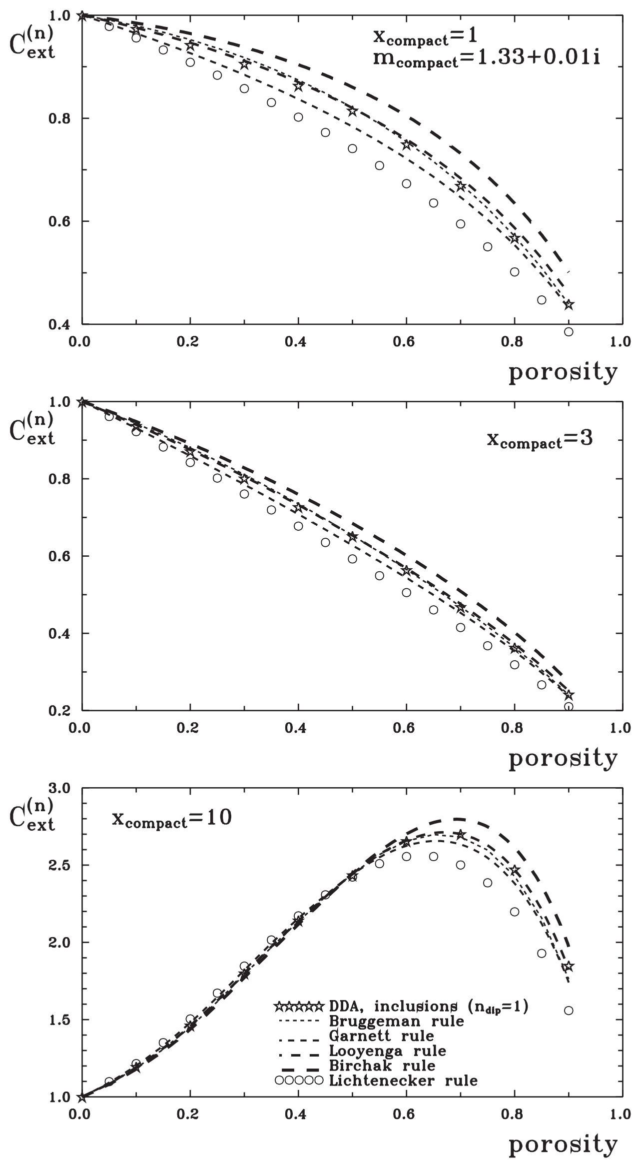

Fig. 2. Porosity dependence of the normalized extinction cross sections calculated for spheres with small inclusions (DDA computations) and with the Lorenz–Mie theory using different EMTs ($m_{\mathrm{compact}} = 1.33 + 0.010i$). The effects of variations of the EMT and particle size are illustrated.

Table 2. Effective Refractive Indices $m = n + ki$ of Porous Particles Calculated Using Different EMTs Presented in Fig. 2[a]

Mixing Rule	Porosity $\mathcal{P} = 0.3$	$\mathcal{P} = 0.5$	$\mathcal{P} = 0.9$
Bruggeman	$1.2284 + 0.0069i$	$1.1611 + 0.0048i$	$1.0310 + 0.0009i$
Garnett	$1.2247 + 0.0066i$	$1.1579 + 0.0045i$	$1.0308 + 0.0008i$
Looyenga	$1.2277 + 0.0068i$	$1.1611 + 0.0048i$	$1.0316 + 0.0009i$
Birchak	$1.2310 + 0.0070i$	$1.1650 + 0.0050i$	$1.0330 + 0.0010i$
Lichtenecker	$1.2210 + 0.0064i$	$1.1533 + 0.0043i$	$1.0289 + 0.0008i$

[a]($m_{\text{compact}} = 1.330 + 0.010i$).

dipoles in DDA terms, the scattering characteristics of aggregates are not well reproduced by the EMT calculations. This fact is illustrated in Fig. 1 where the size dependence of the extinction efficiencies is plotted for two values of particle porosity. For an illustration we choose the Bruggeman EMT.

For particles consisting of cubes containing 27 and 125 dipoles, the difference between the DDA and the Bruggeman-EMT calculations becomes quite large ($\gtrsim$20%) for size parameters $x_{\text{porous}} \gtrsim 10$. In this case the size parameter of the inclusions is 3 and 5 times larger than for simple dipoles. This is enough to modify the pattern of extinction. Larger inclusions produce curves having different slopes from simple dipoles and the Bruggeman-EMT. This conclusion is valid for other factors and other refractive indices.

Note that the mixing rules with non-Rayleigh inclusions were developed within the context of the extended EMT theory (see, for example, the discussion in Ref. 3). For aggregates consisting of inclusions of various sizes (Rayleigh and non-Rayleigh), a model of layered particles can be applied (see the discussion in Ref. 9). Below we consider particles with simple dipole inclusions only.

B. Choice of the Effective Medium Theory

Figure 2 shows the normalized extinction cross sections $C_{\text{ext}}^{(n)}$ for aggregates with small (Rayleigh) inclusions and the effective models based on the Lorenz–Mie calculations with five different EMTs.

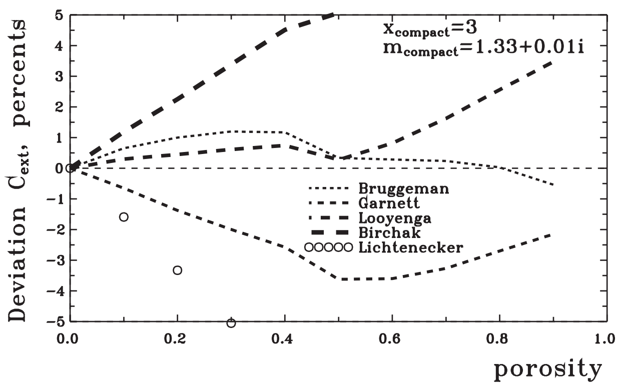

Fig. 3. Dependence of the relative deviations of the extinction cross sections calculated with the DDA and EMT [see Eq. (4)] on the particle porosity. The particle parameters are the same as in Fig. 2 (middle panel).

The normalized cross sections are calculated as

$$C^{(n)} = \frac{C(\text{porous particle})}{C(\text{compact particle of same mass})}$$
$$= (1-\mathcal{P})^{-2/3}\,\frac{Q(\text{porous particle})}{Q(\text{compact particle of same mass})}. \tag{3}$$

They allow one to analyze the role of porosity in particle optics. The quantity $C^{(n)}$ shows how porosity increases or decreases the cross section. The three panels in Fig. 2 provide the results for particles of different masses. For each panel the mass of the particle remains constant but its size increases according

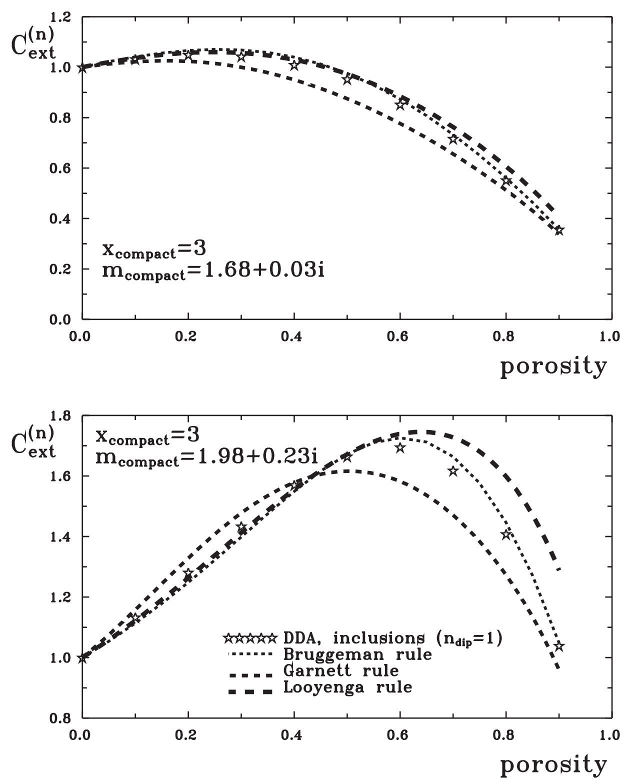

Fig. 4. Porosity dependence of the normalized extinction cross sections calculated for spheres with small inclusions (DDA computations) and with the Lorenz–Mie theory using the three EMTs and two values of m_{compact}. The effect of variations of the EMT and refractive index is illustrated.

to Eq. (2). The refractive index of compact particles is equal to $m_{\mathrm{compact}} = 1.330 + 0.010i$. The refractive indices of porous particles generally decrease with the growth of porosity. Their values are given in Table 2 for three values of $\mathcal{P}$. As follows from Table 2, the difference between the values of m is not large, but it is enough to produce a noticeable difference of the extinction efficiencies especially at large porosity (see Fig. 2). The largest and smallest values of the effective refractive indices (both real and imaginary parts) are obtained from the Birchak and Lichtenecker mixing rules, respectively. Correspondingly, the properties calculated with these *ms* deviate most strongly from the properties for aggregates. We also find the relative deviations in the efficiency factors (in percents) as

$$\text{Deviation} = \frac{Q(\text{EMT-Mie}) - Q(\text{DDA})}{Q(\text{DDA})}\, 100\%. \quad (4)$$

Note that the deviations for particles of different mass and porosity are $\lesssim 5\%$ if the Bruggeman, Garnett, or Looyenga mixing rule is used. However, the deviation becomes $>5\%$ for the Birchak and Lichtenecker rules (see Fig. 3). From Fig. 3 it is seen that the effective models based on the Bruggeman and Looyenga rules reproduce the extinction of aggregates (deviation $\lesssim 1\%$) rather well if $\mathcal{P} \lesssim 0.7$. For larger porosity the Bruggeman model works better. The usage of the Garnett rule leads to deviations within $\sim 4\%$ yielding properties generally smaller than those for aggregates.

Our calculations made for other mixing rules (e.g., quasi-crystalline and coherent potential, see the expressions in Refs. 5 and 18) show that these rules cannot reproduce even the general behavior of the extinction (e.g., $C_{\mathrm{ext}}^{(\mathrm{n})}$ increase with the growth of porosity for $x_{\mathrm{compact}} = 1$). Based on the data presented in Figs. 2 and 3, the three best effective models (with the Bruggeman, Garnett, and Looyenga mixing rules) are chosen for further analysis. The results for these three models and aggregates are shown in Fig. 4. This figure is plotted for one value of $x_{\mathrm{compact}} = 3$ and two values of m_{compact} corresponding to silicate and carbon in the visible part of spectrum. It is seen that the best results are obtained if the model based on the Bruggeman rule is applied. It provides extinctions resembling those of aggregates with small inclusions for particles of different size parameters, porosity, and refractive indices of inclusions. Thus further considerations are made on the models with the Bruggeman rule.

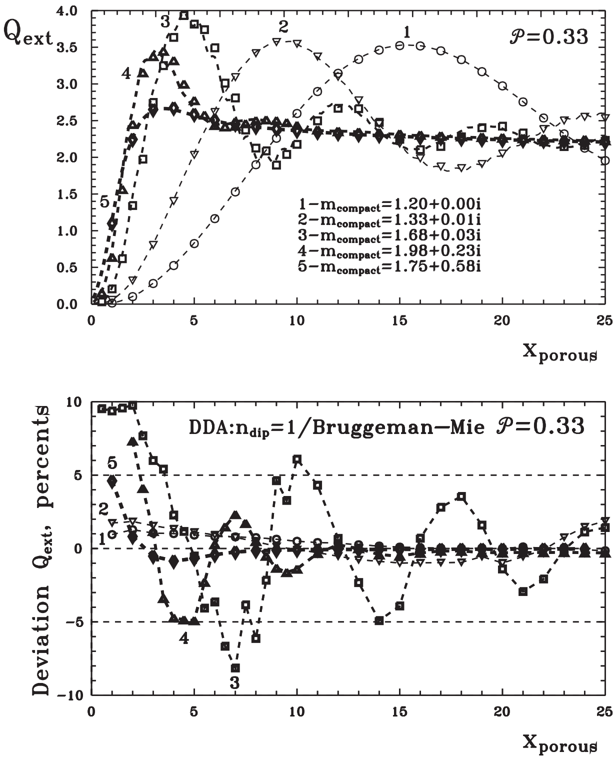

Fig. 5. Size dependence of the extinction efficiency factors (upper panel) calculated for spheres with small inclusions (DDA computations) and with the Lorenz–Mie theory using the Bruggeman EMT. The porosity of the particles is $\mathcal{P} = 0.33$. The effective refractive indices of the porous particles are indicated in Table 3. The lower panel shows the percent difference between the DDA results and the Bruggeman EMT calculations as defined by Eq. (4). The effect of variations of the refractive indices of the inclusions is illustrated.

C. Effect of the Refractive Index of Inclusions

The discussion above is relevant mainly to porous water ice in the visible part of the spectrum. Now

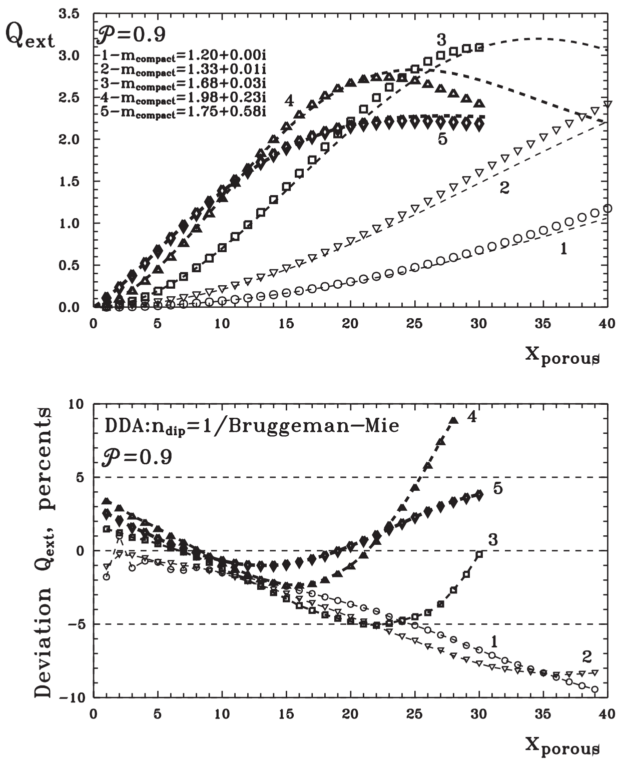

Fig. 6. Same as in Fig. 5 but now for porosity $\mathcal{P} = 0.9$.

Table 3. Effective Refractive Indices $m = n + ki$ of Porous Particles Calculated Using the Bruggeman EMT Presented in Figs. 5 and 6

$\mathcal{P} = 0$	$\mathcal{P} = 0.33$	$\mathcal{P} = 0.9$
$1.2000 + 0.0000i$	$1.1328 + 0.0000i$	$1.0193 + 0.0000i$
$1.3300 + 0.0100i$	$1.2183 + 0.0066i$	$1.0310 + 0.0009i$
$1.6800 + 0.0300i$	$1.4471 + 0.0196i$	$1.0588 + 0.0022i$
$1.9800 + 0.2300i$	$1.6431 + 0.1507i$	$1.0795 + 0.0137i$
$1.7500 + 0.5800i$	$1.4916 + 0.3781i$	$1.0707 + 0.03932$

we consider particles with inclusions of different refractive indices. The comparison between the DDA and the Bruggeman calculations is made in Figs. 5 and 6 for particle porosity $\mathcal{P} = 0.33$ and 0.9, respectively. The upper panels show the extinction efficiency factors' dependence on the size parameter x_{porous}. Five different refractive indices have been considered. The effective refractive indices found with the Bruggeman rule are indicated in Table 3. It is seen that the effective models describe the general behavior of extinction rather well. In all cases the deviations between the factors Q_{ext} found for the aggregate and for the effective models do not exceed ~5% (see the lower panels of Figs. 5 and 6). The exception is the case of silicate particles ($m_{\text{compact}} = 1.680 + 0.030i$) and the porosity $\mathcal{P} = 0.33$. The Lorenz–Mie theory produces the ripple structure of the extinction for these particles. Such a structure does not appear in our DDA calculations. This is because our targets are not smooth spheres but pseudospheres whose cubic inclusions effectively destroy the resonances.

D. Other Factors

We also consider how well the effective model reproduces the scattering (Q_{sca}) and absorption (Q_{abs}) efficiencies, the particle albedo

$$\Lambda = \frac{Q_{\text{sca}}}{Q_{\text{ext}}}, \tag{5}$$

and the asymmetry parameter of the phase function $F(\Theta, \Phi)$:

$$g = \langle \cos \Theta \rangle = \frac{\int_{4\pi} F(\Theta, \Phi) \cos \Theta \, d\omega}{\int_{4\pi} F(\Theta, \Phi) d\omega}. \tag{6}$$

These quantities are plotted in Fig. 7. The comparison is made for the refractive indices of inclusions $m_{\text{compact}} = 1.33 + 0.01i$ and particle porosity $\mathcal{P} = 0.9$. It is seen that the agreement of the results of the DDA and the Bruggeman–Mie computations is rather good. Our calculations performed for other values of $\mathcal{P}$ and m_{compact} show that the effective models better reproduce the extinction properties than the scattering and absorption properties. In the latter case the relative deviation usually does not exceed 10% (in comparison with 5% for extinction). At the same time albedo and the asymmetry parameter are reproduced by the effective models with high accuracy: The relative deviation usually does not exceed 2%.

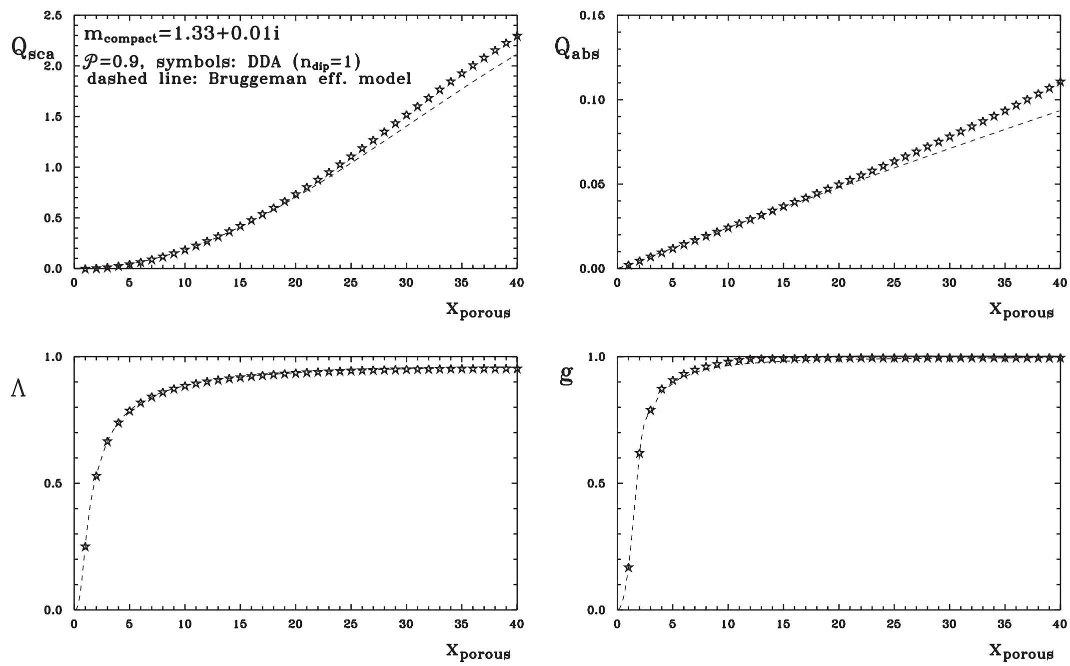

Fig. 7. Size dependence of the scattering (Q_{sca}) and absorption (Q_{abs}) efficiency factors, albedo Λ and the asymmetry parameter g for pseudospheres with small inclusions using DDA computations and the Bruggeman effective model. The refractive indices of inclusions are $m_{\text{compact}} = 1.33 + 0.01i$. The porosity of particles is $\mathcal{P} = 0.9$.

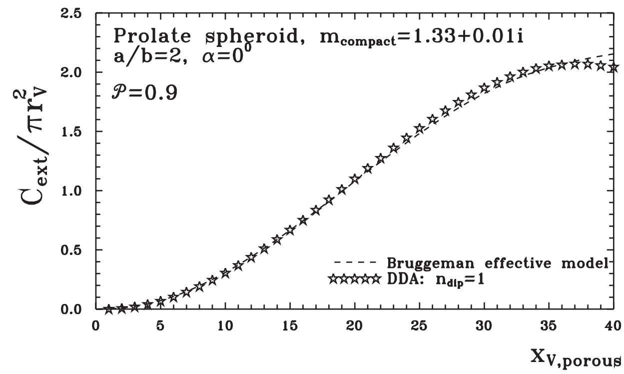

Fig. 8. Size dependence of the extinction efficiency factors calculated for prolate spheroids with small inclusions using DDA computations and the Bruggeman effective model. The refractive indices of inclusions are $m_{\text{compact}} = 1.33 + 0.01i$, and the porosity of particles is $\mathcal{P} = 0.9$. The effect of variations of the particle shape is illustrated.

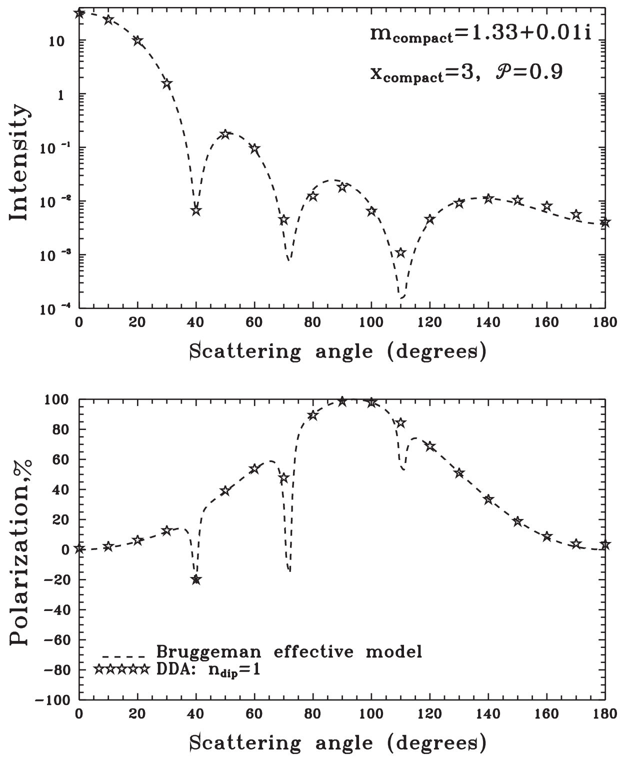

Fig. 9. Intensity and polarization of the scattered radiation calculated for pseudospheres with small inclusions (DDA computations) and effective models (Bruggeman–SVM computations). The refractive indices of the inclusions are $m_{\text{compact}} = 1.33 + 0.01i$, and the porosity of particles is $\mathcal{P} = 0.9$.

E. Effect of the Particle Shape

All previous results have been obtained for fluffy spherical particles that can serve as an approximate model of aggregate particles randomly oriented in space (3D orientation). If the aggregates have a preferential axis of rotation (2D orientation) they can be considered as fluffy axisymmetric particles (e.g., prolate or oblate spheroids).

We perform DDA calculations of the efficiency factors for targets having the shape of prolate spheroids with Rayleigh inclusions. The results are compared with those calculations performed using the separation of variables methods (SVMs) (see Ref. 22) for homogeneous spheroids whose effective refractive index is found from the Bruggeman EMT. Figure 8 shows the size dependence of the extinction efficiencies for prolate spheroids with the aspect ratio $a/b = 2$ for the case of the incident radiation propagating along the rotation axis of the spheroid ($\alpha = 0^0$). Note that for the considered case, the agreement between the DDA and the Bruggeman–SVM computations is even better than for spheres (see Fig. 6): The relative deviations are $\lesssim 4\%$ for $x_{\text{porous}} \lesssim 40$. So the effective models of nonspherical particles seem to improve the accuracy of the effective model computations for aggregates containing small size inclusions.

F. Intensity and Polarization

We also perform illustrative calculations of the intensity and polarization of scattered radiation (see Fig. 9). It is seen that satisfactory agreement between the effective model and the DDA computations is obtained for small and intermediate scattering angles ($\Theta \lesssim 60^0$) only. For larger scattering angles the difference becomes rather large, especially for the second and third minima. This is not unexpected since diffraction plays a major role for small scattering angles, and this depends primarily on the external morphology of the particle. At larger scattering angles, the internal composition plays a larger role. However, the deviations in reproducing these minima are a small concern when we consider a natural polydispersion of particles. In this case, the minima become washed out owing to the polydispersion.

4. Conclusions

We study the general optical behavior of aggregate particles when the porosity increases.

The main results of the paper are the following:

1. The extinction produced by porous pseudospheres with small size (Rayleigh) inclusions can be calculated employing the Lorenz–Mie theory with the refractive index found using the EMT. The deviations that arise using the Bruggeman effective model do not exceed $\sim 5\%$ for particle porosity $\mathcal{P} = 0 - 0.9$ and size parameters $x_{\text{porous}} \lesssim 25$.
2. The effective models represent the behavior of other properties (scattering and absorption efficiencies, particle albedo, asymmetry parameter) quite well and can be used for calculations of the intensity and polarization of the radiation scattered by fluffy aggregates under certain conditions. Preliminary consideration shows that the above conclusions are also valid for spheroidal particles.
3. The effective models can significantly simplify the computations of the optical properties of aggregates containing only Rayleigh inclusions.

We thank Vladimir Il'in and the anonymous reviewers for helpful comments. We thank Bruce

Draine and Piotr Flatau for providing the DDSCAT 6.0 code. This work was supported in part by the TechBase Program on Chemical and Biological Defense, by the Battlefield Environment Directorate under the auspices of the U.S. Army Research Office Scientific Services Program administrated by Batelle (Delivery Order 0395, contract DAAD19-02-D-0001), by grant of the DFG Research Group "Laboratory Astrophysics," and by grants NSh 8542.2006.2, RNP 2.1.1.2152, and RFBR 07-02-00831 of the Russian Federation.

References

1. M. I. Mishchenko, J. Hovenier, and L. D. Travis, eds., *Light Scattering by Nonspherical Particles* (Academic, 2000).
2. C. F. Bohren and D. R. Huffman, *Absorption and Scattering of Light by Small Particles* (Wiley, 1983).
3. P. Chýlek, G. Videen, D. J. W. Geldart, J. S. Dobbie, and H. C. W. Tso, "Effective medium approximations for heterogeneous particles," in *Light Scattering by Nonspherical Particles,* M. I. Mishchenko, J. Hovenier, and L. D. Travis, eds. (Academic, 2000), pp. 274–308.
4. A. H. Sihvola, *Electromagnetic Mixing Formulas and Applications* (Institute of Electrical Engineers, Electromagnetic Waves Series 47, 1999).
5. L. Kolokolova and B. Å. S. Gustafson, "Scattering by inhomogeneous particles: microwave analog experiments and comparison to effective medium theory," J. Quant. Spectrosc. Radiat. Transfer **70,** 611–625 (2001).
6. N. Maron and O. Maron, "On the mixing rules for astrophysical inhomogeneous grains," Mon. Not. R. Astron. Soc. **357,** 873–880 (2005).
7. B. T. Draine, "The discrete dipole approximation for light scattering by irregular targets," in *Light Scattering by Nonspherical Particles,* M. I. Mishchenko, J. Hovenier, and L. D. Travis, eds. (Academic, 2000), pp. 131–145.
8. M. Min, C. Dominik, J. W. Hovenier, A. de Koter, and L. B. F. M. Waters, "The 10 μm amorphous silicate feature of fractal aggregates and compact particles with complex shapes," Astron. Astrophys. **445,** 1005–1014 (2006).
9. N. V. Voshchinnikov, V. B. Il'in, and Th. Henning, "Modelling the optical properties of composite and porous interstellar grains," Astron. Astrophys. **429,** 371–381 (2005).
10. B. T. Draine and P. J. Flatau, *User Guide for the Discrete Dipole Approximation Code DDSCAT.6.0,* astro-ph/0309069, pp. 1–46 (2003).
11. Th. Henning and R. Stognienko, "Porous grains and polarization: the silicate features," Astron. Astrophys. **280,** 609–616 (1993).
12. K. Lumme and J. Rahola, "Light scattering by porous dust particles in the discrete-dipole approximation," Astrophys. J. **425,** 653–667 (1994).
13. M. J. Wolff, G. C. Clayton, P. G. Martin, and R. E. Schulte-Ladbeck, "Modeling composite and fluffy grains: the effects of porosity," Astrophys. J. **423,** 412–425 (1994).
14. A. Doicu and Th. Wriedt, "Equivalent refractive index of a sphere with multiple spherical inclusions," J. Opt. A **3,** 204–209 (2001).
15. P. Mallet, C. A. Guérin, and A. Sentenac, "Maxwell–Garnett mixing rule in the presence of multiple scattering: Derivation and accuracy," Phys. Rev. B **72,** 014205–014209 (2005).
16. M. Kocifaj, M. Gangl, F. Kundracík, H. Horvath, and G. Videen, "Simulation of the optical properties of single composite aerosols," J. Aerosol Sci. **37,** 1683–1695 (2006).
17. Y. Guéguen, M. Le Ravalec, and L. Ricard, "Upscaling: effective medium theory, numerical methods and the fractal dream," Pure Appl. Geophys. **163,** 1175–1192 (2006).
18. N. V. Voshchinnikov, "Optics of Cosmic Dust. I," Astrophys. Space Phys. Rev. **12,** 1–182 (2004).
19. Th. Henning, V. B. Il'in, N. A. Krivova, B. Michel, and N. V. Voshchinnikov, "WWW Database on Optical Constants for Astronomy," Astron. Astrophys. Suppl. sen. **136,** 405–406 (1999).
20. C. Jäger, V. B. Il'in, T. Henning, H. Mutschke, D. Fabian, D. A. Semenov, and N. V. Voshchinnikov, "A database of optical constants of cosmic dust analogs," J. Quant. Spectrosc. Radiat. Transfer **79–80,** 765–774 (2003).
21. H. Chang and T. T. Charalampopoulos, "Determination of the wavelength dependence of refractive indices of flame soot," Proc. R. Soc. London Sen. A **430,** 577–591 (1990).
22. N. V. Voshchinnikov and V. G. Farafonov, "Optical properties of spheroidal particles," Astrophys. Space Sci. **204,** 19–86 (1993).